gravity; H) bed depth; H_f) pressure wave penetration depth; K_v) relative vibrational acceleration; n) likely number of chemical contacts for a particle during vibrational mixing; P_0) environmental pressure; P) half-range for gas pressure pulsations in bed; R) universal gas constant; s) phase slip depth [5]; T) temperature; t) time; t_v) vibration period; v_p) reaction rate; ε) porosity; ρ) particle density; σ) autohesion bond strength; τ_v) phase velocity relaxation time [5]; α) degree of conversion.

LITERATURE CITED

1. A. P. Baskakov, I. E. Kipnis, A. F. Ryzhkov, et al., "Development prospects for fluidization techniques," Abstracts for an All-Union Conference [in Russian], Leningrad (1988), pp. 17-18.
2. Ya. M. Shchelokov, A. M. Avvakumov, and Yu. K. Sazylin, Cleaning Heating Surfaces in Utilizer Boilers [in Russian], Moscow (1984).
3. A. P. Baskakov (ed.), Heat and Mass Transfer in Fluidized Beds [in Russian], Moscow (1978).
4. A. D. Zimon and E. I. Andrianov, Powder-Material Autohesion [in Russian], Moscow (1978).
5. A. F. Ryzhkov and B. A. Putrik, Inzh.-fiz. Zh., 54, No. 2, 188-197 (1988).
6. Ya. B. Geguzin, Sintering Physics [in Russian], Moscow (1984).
7. P. P. Budnikov and A. M. Ginstling, Reactions in Mixtures of Solids [in Russian], Moscow (1971).
8. G. A. Abduragimov, R. P. Meilanov, and Ya. L. Ugai, Inzh.-fiz. Zh., 50, No. 6, 1013-1017 (1986).
9. M. Brown, D. Dollimore, and A. Galway, The Reactions of Solids [Russian translation], Moscow (1983).
10. L. M. Kovba and V. K. Trunov, X-ray Phase Analysis [in Russian], Moscow (1976).
11. A. A. Fotiev, V. L. Volkov, and V. K. Kapustkin, Vanadium Oxide Bronzes [in Russian], Moscow (1978).
12. P. M. Vaisblat and S. L. Komarinskii, Heat and Mass Transfer: International Conference Abstracts, Section 5, Heat and Mass Transfer in Dispersed Systems [in Russian], Minsk (1988), pp. 13-15.
13. O. A. Esin and P. V. Gel'd, The Physical Chemistry of Pyrometallurgical Processes [in Russian], Sverdlovsk (1962).
14. A. K. Ashin and S. T. Rostovtsev, Izv. Vyssh. Uchebn. Zaved., Chernaya Metallurgiya, No. 11, 5-9 (1967).

HEAT TRANSFER AND COMBUSTION FOR A SPIRAL FLOW IN AN IDEAL-DISPLACEMENT REACTOR

I. G. Dik and O. V. Matvienko

UDC 532.542.2:536.25.27:536.46

Hydrodynamic equations have been used with a numerical method to construct the temperature and concentration patterns for a reacting gas. Heat transfer in an ideal-displacement reactor is examined along with the structure of the reaction zone for various values of the spiral flow parameters.

Formulation. Heat transfer, reaction, and ignition in internal flows have various applications [1-6].

The temperature patterns in a reacting flow is related to a considerable extent to the marked temperature dependence of the rate, which governs the flame propagation rate (reaction zone) if the reaction is highly exothermic. Under stationary conditions, the reaction zone propagates upstream as a combustion front. The front is stabilized at a certain distance from the reagent input, at a point dependent on the relation between the input

Kuibyshev Tomsk University.

Translated from Inzhenerno-fizicheskii Zhurnal, No. 2, pp. 217-225, February, 1991. Original article submitted December 4, 1989.

rate and the flame propagation speed [7-9]. At low input rates, the burning region stabilizes close to the inlet on account of heat transfer to the incoming reagent (thermal-conduction state), while at high rates, it stabilizes far away and is formed almost without the involvement of conductive transport (induction mode). The heat transfer through the reactor wall modifies these modes, and a low-temperature transformation may occur [9], when no pronounced hot frontal-type zone is formed. The boundary between the different modes is fairly sharp, which is characteristic of homogeneous flows and ones with velocity gradients of Poiseuille type. In [10], some aspects were discussed of reaction, heat transfer, and ignition in turbulent flows in tubes. Here we present numerical results on how spiraling affects heat transfer and combustion in a tube.

Spiral flows are of interest because of their special features, which have been surveyed [5, 7]. In a strongly spiraling flow, there are considerable pressure gradients, which can lead to a recirculation zone. That zone with extensive vorticity in a reacting flow tends to stabilize the flame by transferring heat from the circulating combustion products. The increased mixing rate at the boundary of that zone tends to reduce the flame length. Spiraling should therefore affect the reactor characteristics, in particular the thermal stress.

The model is based on current-function variables and vorticity. The pressure is excluded as an explicit variable and there is automatic check on the mass conservation downstream. For an incompressible stationary flow with constant viscosity,

$$\begin{aligned}
&\xi^2\,\mathrm{Re}/4\left\{\frac{\partial}{\partial x}\left[\frac{\omega}{\xi}\frac{\partial\psi}{\partial\xi}\right]-\frac{\partial}{\partial\xi}\left[\frac{\omega}{\xi}\frac{\partial\psi}{\partial x}\right]\right\}-\\
&-\left\{\frac{\partial}{\partial x}\left[\xi^3\frac{\partial\omega/\xi}{\partial x}\right]+\frac{\partial}{\partial\xi}\left[\xi^3\frac{\partial\omega/\xi}{\partial\xi}\right]\right\}-\mathrm{Re}\,\xi\frac{\partial v_\varphi^2}{\partial x}=0,\\
&\mathrm{Re}/4\left\{\frac{\partial}{\partial x}\left[v_\varphi\xi\frac{\partial\psi}{\partial\xi}\right]-\frac{\partial}{\partial\xi}\left[v_\varphi\xi\frac{\partial\psi}{\partial x}\right]\right\}-\\
&-\left\{\frac{\partial}{\partial x}\left[\xi\frac{\partial v_\varphi\xi}{\partial x}\right]+\frac{\partial}{\partial\xi}\left[\xi\frac{\partial v_\varphi\xi}{\partial\xi}\right]\right\}+2\frac{\partial v_\varphi\xi}{\partial\xi}=0,\\
&\frac{\partial}{\partial x}\left[\frac{1}{\xi}\frac{\partial\psi}{\partial x}\right]+\frac{\partial}{\partial\xi}\left[\frac{1}{\xi}\frac{\partial\psi}{\partial\xi}\right]+\omega=0.
\end{aligned}\tag{1}$$

Here x is the longitudinal coordinate, which is referred to the tube radius r, ξ the dimensionless radial coordinate, and v_φ the dimensionless tangential velocity, whose scale is evident from the boundary conditions. The same applies to the current function ψ, which is used in formulating the axial and radial velocity components:

$$v_x=\frac{1}{2\xi}\frac{\partial\psi}{\partial\xi},\quad v_\xi=-\frac{1}{2\xi}\frac{\partial\psi}{\partial x},\tag{2}$$

as well as the tangential component of the vortex stress

$$\omega=2\left(\frac{\partial v_\xi}{\partial x}-\frac{\partial v_x}{\partial\xi}\right).\tag{3}$$

It has been assumed in setting the boundary conditions that the velocity distribution at the inlet corresponds to the rotation of a solid:

$$x=0:\ \psi=\xi^2,\ \omega=0,\ v_\varphi=\sigma\xi.\tag{4}$$

In (4), $\sigma=\Omega r/U$, Ω is the angular velocity at the inlet, and U the rate at which the substance is supplied. In addition to σ, there is the hydrodynamic characteristic $\mathrm{Re}=2Ur/\nu$, in which ν is the kinematic viscosity.

Mild boundary conditions are set at the outlet, which simulate free outflow:

$$x=L:\ \frac{\partial^2\psi}{\partial x^2}=0,\ \frac{\partial^2\omega}{\partial x^2}=0,\ \frac{\partial^2 v_\varphi}{\partial x^2}=0.\tag{5}$$

At the tube wall, the attachment condition and the constant flow rate give

$$\xi=1:\ \psi=1,\ v_\varphi=0.\tag{6}$$

Symmetry conditions apply at the axis:

$$\xi = 0:\ \psi = 0,\ v_\varphi = 0. \tag{7}$$

The vortex stress at the axis and wall may be determined by the [12] method.

The equations for the temperature and concentration patterns are written on the assumption of first-order exothermic reaction:

$$\frac{\mathrm{Re\,Sc}}{4}\left\{\frac{\partial}{\partial x}\left[\eta\frac{\partial\psi}{\partial\xi}\right]-\frac{\partial}{\partial\xi}\left[\eta\frac{\partial\psi}{\partial x}\right]\right\}-\left\{\frac{\partial}{\partial x}\left[\xi\frac{\partial\eta}{\partial x}\right]+\right.$$
$$\left.+\frac{\partial}{\partial\xi}\left[\xi\frac{\partial\eta}{\partial\xi}\right]\right\}-\xi\,\mathrm{Da}\,(1-\eta)\exp\left(\frac{\theta-\Theta_a}{1+\beta\,(\theta-\Theta_a)}\right)=0,$$
$$\frac{\mathrm{Re\,Pr}}{4}\left\{\frac{\partial}{\partial x}\left[\theta\frac{\partial\psi}{\partial\xi}\right]-\frac{\partial}{\partial\xi}\left[\theta\frac{\partial\psi}{\partial x}\right]\right\}-\left\{\frac{\partial}{\partial x}\left[\xi\frac{\partial\theta}{\partial x}\right]+\right. \tag{8}$$
$$\left.+\frac{\partial}{\partial\xi}\left[\xi\frac{\partial\theta}{\partial\xi}\right]\right\}-\xi\,\mathrm{Da\,Le^{-1}}\Theta_a\,(1-\eta)\exp\left(\frac{\theta-\Theta_a}{(1+\beta\,(\theta-\Theta_a)}\right)=0.$$

Here η is the reagent burnup, $\theta = T - T_0/T^* (- E/RT^*)$, $T_* = T_0 + Q/c\rho$ the adiabatic reaction temperature, T_0 the inlet temperature, and $Q/c\rho$ the adiabatic temperature rise. Equation (8) contains some new parameters: $\mathrm{Pr} = \nu/\kappa$, $\mathrm{Sc} = \nu/D$, $\mathrm{Le} = D/\kappa$, which reflect the relation between the viscosity ν, thermal conductivity κ, and diffusion coefficient D. The maximum temperature rise is $\theta_a = Q/c\rho\ E/RT_*^2$. The reaction rate is governed by the Damkeller parameter $\mathrm{Da} = k(T_*)r^2/D$, in which $k(T_*)$ is the characteristic reaction rate, which is related to the stearic factor by $k(T_*) = k_0 \exp(-E/RT_*)$. The rate is sensitive to temperature on account of $\beta = RT_*/E$. For combustion, $\beta \ll 1$.

The boundary conditions in (8) are fairly obvious:

$$\eta\,(0,\ \xi)=0,\ \ \theta\,(0,\ \xi)=0;\ \ \left.\frac{\partial^2\eta}{\partial x^2}\right|_{x=L}=0,\ \ \left.\frac{\partial^2\theta}{\partial x^2}\right|_{x=L}=0;$$
$$\left.\frac{\partial\eta}{\partial\xi}\right|_{\xi=0}=0;\ \ \left.\frac{\partial\theta}{\partial\xi}\right|_{\xi=0}=0;\ \ \left.\frac{\partial\eta}{\partial\xi}\right|_{\xi=1}=0,\ \ \theta\,(x,\ 1)=0. \tag{9}$$

This is a multiparameter problem, where the parameters may be divided into four groups.

1. Re and σ are hydrodynamic parameters characterizing the flow structure. Calculations for $\sigma \le 4$ and $10^2 \le \mathrm{Re} \le 10^3$ show that the changes in the axial and tangential velocity components and in the temperature and concentration as Re varies amount to a coordinate transformation that alters the longitudinal coordinate x by a factor Re, since the equations are slightly elliptic (in other words, the small contribution from flows of molecular type for large Re). If there is strong spiraling and a recirculation zone, that transformation is incorrect, but the pictures for the flow, reaction, and heat transfer are not qualitatively altered. The quantitative changes are slight, so no analysis for the Re effects is given below. The major parameter is taken as σ.

2. Pr, Sc, and Le describe the transport features, with the main caluclations performed with all of them taken as one.

3. Da, Θ_a, and β are reaction parameters; β is characteristically about $5\cdot10^{-2}$. The other thermal energy parameters were varied in the following ranges in the calculations: Θ_a from 5 to 15 and Da from 10^3 to 10^5. The Frank-Kamenetskii number is important:

$$\mathrm{Fk} = \Theta_a\,\mathrm{Le^{-1}\,Da}\exp\left[-\frac{\Theta_a}{1-\beta\Theta_a}\right],$$

as it characterizes the heat production rate at the initial temperature T_0. Thermal-explosion theory shows [12] that various thermal conditions are set up for the various Fk: low-temperature and high-temperature ones. The reaction at small Fk produces a slight temperature rise, with the flow showing thermal stabilization. At high Fk, the reaction produces an explosive temperature increase, so the reagent ignites.

4. The apparatus parameter L is the dimensionless reactor length. It was taken as fairly large (L = 100). For L > 100, its effects on the heat-transfer and flow characteristics are minor.

Then the treatment is essentially a three-parameter one, namely based on σ, Da, and Θ_a.

Method. System (1)-(9) was solved by a finite-difference method [11] of simple but universal type on a net uneven in both coordinates, with closer spacing at the inlet and the tube wall. The finite-difference analog of those partial differential equations is a system of nonlinear algebraic equations, which was solved by the Gauss–Seidel method.

Iteration convergence for $\sigma \geq 3$ was provided by lower relaxation for the tangential vortex stress component ω/ξ. Internal iterations by Newton's method were used to derive the temperature distribution. The convergence criterion was

$$|\varphi^{(N)} - \varphi^{(N-1)}| < 10^{-3}|\varphi^{(N)}|,$$

in which Φ is a vector having components $\Phi = (\omega/\xi, \psi, v\ \xi, \eta, \theta)$; and N is the iteration number.

The axial and radial velocity components were derived by numerical differentiation of the current function on a three-point scheme via (2).

Hydrodynamics. We neglected the temperature dependence of the viscosity, which enabled us to decouple the hydrodynamic treatment from the thermal and diffusion ones. The (1) equations of motion with appropriate boundary conditions were solved without reference to the others, as they define all the hydrodynamic features, against which background and largely due to which one gets the features in the heat transfer and reaction. Therefore, the hydrodynamic description should precede the analysis of the thermal-kinetic part.

For small σ (up to $\sigma \approx 1$), the effects of the spiraling on the velocity distribution are slight. For $\sigma > 2$, the centrifugal forces result in a region of reduced pressure at the axis. There is thus a dip in v_x near it, which is formed near the inlet, at which point the interaction with the wall has already given rise to boundary layers but the tangential velocity component is still quite large. For $\sigma > 6$, the pressure gradients increase to such an extent that a recirculation zone is formed, whose size and shape are governed by Re and σ, as is the intensity of the reverse flows there.

Flow retardation or even reversal near the axis leads to increase in v_x at the periphery. The v_x pattern has a maximum at $\xi = \xi_m$. As σ increases, so does the maximum v_x, and ξ_m is displaced towards the wall (Fig. 1).

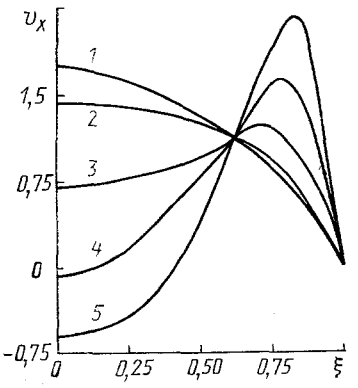

Fig. 1

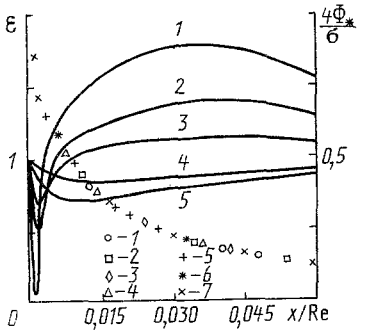

Fig. 2

Fig. 1. Radial distribution of the axial velocity in the x = 3 section for various spiraling parameters (Re = 160): σ = 0(1); 2(2); 4(3); 6(4); 9(5).

Fig. 2. Variation in spiraling intensity $4\Phi_*/\sigma$ and relative coefficient ε representing the heat transfer downstream in the flow. For $4\Phi_*/\sigma$: 1) σ = 3, Re = 160; 2) 6 and 160; 3) 9 and 160; 4) 4 and 160; 5) 4 and 320; 6) 4 and 640; 7) 4 and 800; for ε: Re = 160; Da = $5 \cdot 10^4$; Θ_a = 76.5; σ = 9(1), 6(2), 4(3); Θ_a = 10, σ = 4(4), 6(5).

The following integral parameter characterizes the spiraling intensity:

$$\Phi_* = \frac{\int_0^1 v_\varphi v_x \xi^2 d\xi}{\int_0^1 v_x^2 \xi d\xi}.$$

It is clear that $\Phi_*(0) = \sigma/4$. Figure 2 shows $4\Phi_*/\sigma$ as a function of x/Re for various σ and Re, which indicate that all the calculated points lie on a single curve. The highest spiraling intensity is near the inlet. Downstream, frictional forces cause the spiraling to degenerate ($\Phi_* \approx 0.1\ \Phi_*(0)$ for $x \approx 0.1$ Re), and one gradually gets a velocity profile corresponding to a Hagen–Poiseuille section.

The flow retardation at the wall leads to material being displaced from the periphery towards the axis, and the more so the larger σ. For $\sigma > 6$, v_ξ exceeds the radial velocity for $\sigma = 0$ by an order of magnitude.

The convective momentum, matter, and heat transport in the spiral flow in the radial direction may thus become substantial, which favors vigorous mixing and the establishment of more uniform η and θ profiles.

Heat Transfer. The heat transfer trends in a reacting medium are related to the reaction state.

If the heat production rate is low, thermal stabilization sets in at a certain distance from the inlet: a parabolic temperature profile is set up that is independent of x, and the mean temperature over the flow $\langle\Theta\rangle = 2\int_0^1 \Theta v_x \xi d\xi$ tends axymptotically to $\Theta_s \approx Fk/6$, which is much less than Θ_a. The reagent concentration alters only slightly with flow self-heating in the low-temperature mode, so the Arrhenius heat source can be represented as a source with constant output Fk. The temperature patterns and thus the heat flux to the wall and the heat-transfer criterion differ from those when one incorporates the temperature dependence of the source by not more than 10%. The heat-transfer criterion is almost independent of Fk and Da, as in a spiral flow with a constant heat source [13].

The temperature pattern is related to the velocity one. In particular, for a straight flow and adiabatic wall, the maximum temperature in a flow containing a bulk heat source will occur at the wall, where $v_x = 0$. With a thermally conducting wall, the heat transfer reduces the temperature in the wall region. Therefore, the maximum temperature in an x = const section will occur at $\xi = \xi t < 1$. Away from the inlet, the point with the maximum temperature shifts towards the axis.

The spiraling increases the flow rate in the wall region, which means that fresh unheated material is more vigorously transferred towards the cold wall, which reduces the temperature there and smooths the temperature profile while reducing the heat flux to the wall $q = \partial\theta/\partial\xi|_{\xi=1}$. The flow retardation at the axis as the spiraling increases means that the temperature there rises. For large σ, the recirculation zone results in a region into which the unreacted material is drawn, whose reaction occurs under conditions of recirculation, which results in a maximum on the $\theta(0, x)$ curve for $\sigma = 9$ near the inlet. Downstream, where centrifugal-force effects weaken, the temperature curves corresponding to the various σ converge.

The temperature rise near the axis with spiraling is compensated by the reduction near the wall, so there is only a slight increase in $\langle\Theta\rangle$. The spiraling affects the temperature pattern in such a way that $Nu = q\langle\Theta\rangle$ is reduced as σ increases. Figure 2 shows the change in the relative heat-transfer criterion $\varepsilon = Nu(\sigma)/Nu(0)$. The minimal ε occurs in sections where the centrifugal forces are large. Downstream, as the spiraling degenerates, $\varepsilon \to 1$.

In the other limiting case, rapid heat production, ignition and combustion occur in a certain section x_*; this substantially influences $\varepsilon(x)$, as shown in Fig. 2 (curves 1-3). In the initial part, the spiraling acts as in the low-temperature mode, namely ε falls as σ increases. For $x > x_*$, the high-temperature reaction ceases, and ε increases with σ, the more so the stronger the reaction (the larger Da and Fk). For $x > x_*$, the interest attaches to how the spiraling affects the heat transfer for a chemically inert flow [14].

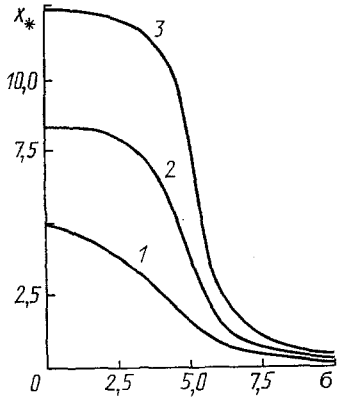

Fig. 3

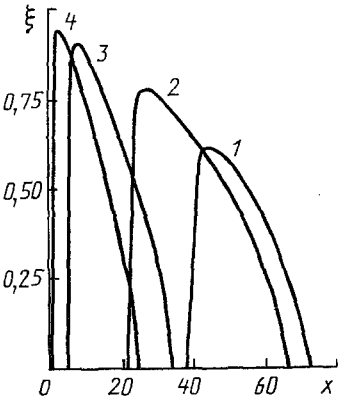

Fig. 4

Fig. 3. Coordinate of the ignition cross section as a function of spiraling parameter: Re = 160; Θ_a = 7.5; Da = $2\cdot10^4$ (1), $1.25\cdot10^4$ (2), $1\cdot10^4$ (3).

Fig. 4. Boundaries to reaction zone for various spiraling parameters: Re = 160; Θ_a = 7.5; Da = 10^4; σ = 0(1); 4(2), 6(3); 9(4).

The ignited material has a temperature about equal to the adiabatic burning temperature, which greatly exceeds the wall temperature, so there are large temperature gradients, particularly in the radial direction. The spiraling accelerates the mixing, and convective radial transport is important. Consequently, the cold material from the wall reaches the axis, which cools the flow and reduces $\langle\Theta\rangle$. The variation in temperature gradient at the wall with the spiraling is more complicated. For $x > x_*$, q is reduced because of the vigorous cooling. However, the reduction in $\langle\Theta\rangle$ as the spiraling increases for a given x is more pronounced, and Nu increases.

Ignition and Combustion. As the reaction intensifies (Fk increases), the heat transfer at the wall ceases to balance the heat production in the flow. The temperature dependence of the heat production rate becomes important. The thermal-stabilization condition may be written as

$$\mathrm{Nu}_s\langle\Theta\rangle = \mathrm{Fk}\exp(\langle\Theta\rangle),$$

to derive the critical value $\mathrm{Fk}_* = \mathrm{Nu}_s/\exp(1)$. The calculations give Nu_s, the heat-transfer number for a constant source, of 3.0, so the estimate for Fk_* is 1.10. The critical conditions for spiral and straight flows are identical, since it is assumed that the ignition occurs far from the inlet, where the spiraling has completely degenerated.

The ignition mechanism is very much dependent on σ; at low values, it occurs because the mixture is heated by the exothermic reaction. At higher values, a recirculation zone occurs, and the ignition mechanism alters if the reaction is vigorous enough: instead of self-ignition, there is ignition caused by the hot combustion products from the recirculation zone, whose temperature is close to Θ_a, while the extent of reaction tends to one. The maximum temperature in a section is attained at the boundary of the recirculation zone (along the isotach $v_x = 0$).

The ignition and combustion occur at $x = x_*$, where $\langle\Theta\rangle$ attains its maximum value. Figure 3 shows how x_* varies with σ for various Da.

If σ = 0, a weak reaction (but with $\mathrm{Fk} > \mathrm{Fk}_*$) results only in an induction state with large x_*. High values, with the recirculation zone, may increase the particle paths considerably, so x_* approaches the inlet.

With a strong reaction, even for σ = 0, the combustion occurs in the thermal-conduction mode at a short distance from the inlet. The preflame zone may actually be reduced by increase in σ, particularly for those Da where the ignition occurs near the recirculation zone. For large Da, the reduction in x_* as σ increases is fairly smooth. At moderate values (but such that $\mathrm{Fk} > \mathrm{Fk}_*$), the transition from one mode to another is fairly sharp in the form of critical conditions.

It is insufficient to characterize the combustion zone only from the maximum in $\langle\theta\rangle$; the combustion does not occur uniformly throughout the cross section, as heat transfer at the wall interferes. The combustion region is also extended in x. The heat transfer means that the temperature never attains the θ_a. The reaction zone is the region where the temperature is not less than $\theta_a/2$. An increase in σ causes retarded or even reversed flow, and the reduced heat transfer brings the boundary of the reaction zone close to the wall and raises the maximum temperature there. The reaction zone is then displaced towards the inlet, as Fig. 4 shows.

Spiraling thus increases the thermal stress on the reactor.

Notation. v_x) axial velocity; v_ξ) radial velocity; η) product concentration; θ) dimensionless temperature; σ) spiraling parameter; ψ) current function; ω) vortex stress; Re) Reynolds number; Sc) Schmidt number; Le) Lewis number; Nu) Nusselt number; Da) Damkeller number; Fk) Frank–Kamenetskii parameter.

LITERATURE CITED

1. B. P. Ustimenko, K. B. Dzhakupov, and V. O. Krol', Simulating the Aerodynamics and Combustion in Furances and Engineering Devices [in Russian], Alma Ata (1986).
2. Z. Skassia and A. Kennedy, Raket. Tekh. Kosmonavtika, 12, No. 9, 130-136 (1974).
3. V. K. Baev, V. I. Golovachev, and V. A. Yasakov, Two-Dimensional Turbulent Reacting-Gas Flows [in Russian], Novosibirsk (1976).
4. E. I. Maksimov, N. I. Peregudov, and A. A. Butakov, Fiz. Goreniya Vzryva, No. 4, 895-898 (1975).
5. V. K. Shchukin and A. A. Khalatov, Heat Transfer, Mass Transfer, and Hydrodynamics in Spiral Flows in Axisymmetric Channels [in Russian], Moscow (1987).
6. D. Lilly, Raket. Tekh. Kosmonavtika, 15, No. 8, 8-12 (1977).
7. A. Gupta, D. Lilly, and N. Saired, Spiral Flows [Russian translation], Moscow (1987).
8. A. G. Merzhanov and A. K. Filonenko, Dokl. Akad. Nauk SSSR, 152, No. 1, 143-146 (1963).
9. R. M. Zaidel' and Ya. B. Zel'dovich, Zh. Prikl. Mat. Tekhn. Fiz., No. 4, 27-32 (1963).
10. I. G. Dik and O. V. Matvienko, Inzh.-fiz. Zh., 54, No. 5, 860 (1988).
11. A. D. Gosman, V. V. Pan, A. C. Ranchel, Numerical Methods of Researching Viscous-Liquid Flows [Russian translation], Moscow (1972).
12. D. A. Frank–Kamenetskii, Diffusion and Heat Transfer in Chemical Kinetics [in Russian], Moscow (1987).
13. O. V. Matvienko, Current Topics in Thermophysics and Physical Hydrodynamics [in Russian], Novosibirsk (1987), pp. 82-83.
14. I. G. Dik and O. V. Matvienko, Izv. Sib. Otd. Akad. Nauk SSSR, Ser. Tekhn. Nauk, No. 3, 40-43 (1989).